INTERNATIONAL JOURNAL OF HYDROGEN ENERGY 46 (2021) 28925–28935

Available online at www.sciencedirect.com

ScienceDirect

journal homepage: www.elsevier.com/locate/he

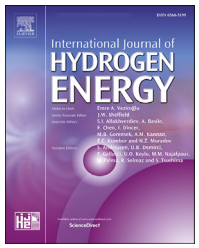

Discriminating between the effect of pulse width and duty cycle on the hydrogen generation performance of 3-D electrodes during pulsed water electrolysis

*Fernando Rocha, Joris Proost**

Division of Materials and Process Engineering, Université Catholique de Louvain, 1348 Louvain-la-Neuve, Belgium

HIGHLIGHTS

- The current during a pulse on-time is higher than the current of DC electrolysis.
- During the off-time of a pulse, a change in polarization is observed.
- Pulses with a 50% duty cycle and widths <1 ms are mainly capacitive.
- Pulses with a 99% duty cycle result in an increase in average current.
- Forced electrolyte flow has a positive effect on faradaic pulses.

ARTICLE INFO

Article history:
Received 30 July 2020
Received in revised form
24 November 2020
Accepted 25 November 2020
Available online 15 December 2020

Keywords:
Pulsed power
Water electrolysis
3-D electrodes
Hydrogen production

ABSTRACT

The present study investigates the effect of applying voltage and current pulses during alkaline water electrolysis using 3-D Ni-based electrodes. The pulses had a square shape and alternated hydrogen production and resting time. When voltage pulses were applied, it was observed that the current at on-time was systematically higher than the current during DC electrolysis. However, during off-time, a change in polarization was observed, which decreased the overall voltage pulse performance. For pulses with a 50% duty cycle and a pulse width of 1 ms, the current response was mainly capacitive and almost no hydrogen production occurred. Current pulses on the other hand were proven to be much more promising in improving the energetic process efficiency. In that case, a pulse period of 2 ms resulted in an overpotential reduction of 17% for a 50% duty cycle. This reduction further increased to 28% when decreasing the duty cycle to 20%. Finally, in all cases where faradaic processes were dominant, applying a forced electrolyte flow was shown to be beneficial.

* *Corresponding author.*
E-mail address: joris.proost@uclouvain.be (J. Proost).
https://doi.org/10.1016/j.ijhydene.2020.11.232

Introduction

It is a scientific consensus that anthropogenic activities are the main causes of global warming [1]. By the end of the past century, global temperature has increased by 0.6° relative to the pre-industrial climate. This raise is mainly a consequence of carbon dioxide emissions from the burn of fossil fuels. As a response, in 2015 195 countries signed the Paris Agreement to reduce CO_2 emissions to limit global warming to below 2° [2]. With global warming threatening environmental safety, substitutes for fossil fuels must emerge. One possibility is to use hydrogen gas as a fuel for transportation, industry, and house heating. The advantages of using hydrogen include that (i) it has the highest energy density of any known fuel, (ii) the only exhaust product is water at conversion to energy, (iii) it is non-toxic, and (iv) it is sustainable [3]. However, unlike fossil fuels, hydrogen gas is not readily found on Earth. This is a consequence of the low density of this substance, so that the gravitational field of our planet is not high enough to keep it [4]. On the other hand, the element hydrogen is present in many chemical compounds and it is the most abundant element on the universe [5]. Therefore, hydrogen gas can be produced through chemical reactions. In this condition, hydrogen works as an energy carrier, just like electricity [6]. Hence, it can be produced to store energy from renewable and clean sources, which are intrinsically variable and intermittent. As a consequence, the increase in their penetration in the energy grid demands a large-scale energy storage system. It is in this context that hydrogen becomes essential [7]. The method that allows hydrogen production using the electrical energy coming from green sources is called water electrolysis. It is a mature technology based on the application of a direct current to an aqueous electrolyte to dissociate it into hydrogen and oxygen gas. The hydrogen produced in this way has a high purity that can reach up to 99.999 vol% [8]. Despite its environmental advantages, electrolytic hydrogen is not yet widely used as a consequence of its production cost, still more elevated than other techniques/fuels [9]. As a result, water electrolysis still needs research efforts to reach economic viability [10].

Within these efforts, some promising studies have shown an improvement in the hydrogen generation performance of water electrolysis by the substitution of DC (direct current) by a pulsed power supply. For instance, Vanags et al. have published some articles about inductive pulsed water electrolysis [11]. This group created a set-up with inductive voltage pulses that could enhance hydrogen production efficiency. The system consisted of two electric circuits. In the first, a pulsed voltage was created by the on/off switching of a transistor. A coil in the first circuit then induced a voltage pulse in the coil of the second circuit. The resulting induced voltage pulse had a high voltage and a short width followed by a long tail. The authors explained that at the first stage, the double layer was charged and the cell worked as a capacitor with a high charging factor. Then, the energy accumulated was discharged slowly through water electrolysis, with an enhanced process efficiency. Shimizu et al. [12] also used inductive voltage pulses as a way to improve the process efficiency. These authors claimed that in their system, electrolysis was controlled by electron transfer, and not by diffusion as in conventional DC water electrolysis. Demir et al. [13] used transistors to create voltage pulses. According to these authors, the application of pulses facilitated the removal of bubbles from the electrode surface, hence improving the electrolysis performance by increasing the electrode active surface area. Huang et al. [14] in turn used current pulses during the electrolysis of aqueous ammonium sulfite solutions to produce hydrogen gas. Their results showed a better efficiency for pulsed electrolysis as well. Lin et al. [15] observed higher currents densities for pulsed voltage electrolysis. According to these authors, this was a result of the acceleration in bubble movement and improved mass transfer. Dobó et al. studied the impact of current [16] and voltage [17] fluctuations on the water electrolysis efficiency. The authors observed a loss in performance with current fluctuations. Voltage fluctuations, on the other hand, showed a better performance under specific conditions.

The use of pulsed power has also been studied extensively in electrochemical applications other than water electrolysis. For instance, Chao et al. [18] have studied pulsed discharge electrolysis for the degradation of organic compounds for wastewater treatment. Their results showed a reduced energy cost of the process using pulses. Othmani et al. [19] has studied the substitution of a direct current by an alternate current during the anodic oxidation of organic compounds in wastewaters. These authors observed an increase in the electrode's lifetime and a decrease in energy consumption.

A more generic interest in the use of pulsed power is related to the intermittent nature of renewable sources, which implies that electrolyzers must handle frequent start-stop cycles and allow partial load operations. In this context, Siracusano et al. [20] studied the effect of load and thermal cycles at high current densities (3 A/cm^2) in a membrane-electrode assembly based on a proton exchange membrane (PEM) and low catalyst loadings. Galvanostatic cycles of 2 s, 10 s, and 1800 s were studied. The authors observed an increase in voltage over time at direct current due to the accumulation of gases within the electrode micropores and due to the modification of the oxidation state at the anode surface. This voltage increase was lower for cycled operation due to bubble escape and catalyst regeneration at the rest (zero-current) stage. Furthermore, a more pronounced membrane thinning was observed when direct current was used.

Along the same lines, in view of a better managing of unstable power inputs coming from renewable sources which my result in hydrogen/oxygen gas mixing, there is an increasing interest in decoupling the hydrogen evolution (HER) from the oxygen evolution reaction (OER), so that they can occur at different times. In this respect, Symes and Cronin [21] introduced the concept of electron-coupled-proton buffers (ECPB) to separate the two water electrolysis half-reactions. In a first step electricity was used to oxidize water, while protons and electrons were stored in a solution containing the ECPB (phosphomolybdic acid in their case). Then, the reduced ECPB was re-oxidized and protons were reduced, producing hydrogen. This method prevented gas mixing and increased the equipment flexibility with respect to the choice of the membranes and electrode materials. An interesting application of such ECPB's is that solar energy

could then be used to produce hydrogen during the day while during the night windmills would be producing oxygen [22].

Still in order to facilitate gas separation and to deal with variable energy inputs, Rausch et al. [23] developed an electrolysis system with a redox mediator to decouple the two water electrolysis half-reactions. In their case, water was oxidized at the same time a redox mediator (silicotungstic acid) was reduced. Then, the solution containing the reduced redox-mediator was transferred to a chamber containing catalysts for spontaneous hydrogen evolution. With this method, the HER was no longer coupled to the OER, increasing the rate of H_2 evolution by a factor of 30 compared with state-of-the-art PEM electrolyzers. Chen et al. [24] used nickel hydroxide ($Ni(OH)_2$/NiOOH) as a redox mediator in a set-up without any membrane. In the first step, electricity was used to reduce water and to oxidize $Ni(OH)_2$. After that, the power supply was used to reduce NiOOH and to oxidize the hydroxyl ion. This system could also be coupled with a zinc anode to form a NiOOH–Zn battery to produce H_2 during electrolysis and to provide electricity during battery discharge. Coupling this system with solar panels, one could imagine a hydrogen production at noon (higher power input) and oxygen production at dusk. Alternatively, during the day, hydrogen could be produced and the discharge of the NiOOH–Zn battery could provide electricity during the night. The same solid-state nickel (oxy)hydroxide redox mediator was used by Dotan et al. [25]. They created a membrane-free two electrodes electrolyzer set-up. The authors claimed to have improved the energy efficiency of the decoupled process using cobalt additives to catalyze the $Ni(OH)_2$/NiOOH reaction and inhibit oxygen evolution during HER. In their set-up, hydrogen was produced at a platinized nickel-coated stainless-steel cathode at the same time that a $Ni_{0.9}Co_{0.1}(OH)_2$ anode was oxidized to $Ni_{0.9}Co_{0.1}OOH$. Then, a solution of hot electrolyte (95 °C) was circulated in the cell, causing the reduction of $Ni_{0.9}Co_{0.1}OOH$ and oxygen production. Photoelectrochemical cells have been tested as well in an ECPB decoupled system [26]. Moreover, redox mediators can also be used to drive chemical reactions other than HER/OER in the other half-cell. For instance, Xiao et al. [27] created a battery at which oxygen was produced during charging and hydrogen at the discharge in a dual-electrolyte set-up having FeO_x as redox-mediator.

Finally, using a decoupled system with MnO_2 as a redox mediator, Vincent et al. [28] claimed to have achieved a better efficiency by a decrease in the diffusion layer thickness, caused by the quick alternation in the hydrogen/oxygen production (alternation period between 2 and 200 ms). Frensch et al. [29] studied the influence of the operation mode in the degradation of a proton-exchange membrane for water electrolysis. Among the analyzed options were constant current, constant voltage, and constant cycling operations. The latter consisted of current pulses switching between 0 and 2.0 A/cm^2 with a 50% duty cycle and relatively large pulse widths of 10, 60, and 100 s, chosen because close to a solar PV power profile. It was found that faster dynamic cycles improved the cell performance due to a decrease in total ohmic resistance. The authors suggested as possible explanation that the observed decrease in cell potential resulted from an acceleration of bubble detachment and a change in bubble growth behavior, reducing both cell resistance and membrane dehydration.

Returning to more classical water electrolysis, which is the topic of interest for the current paper, Rakousky et al. [30] observed an increase in cell voltage over time (time scale of 1000 h). Around 60% of the observed increase was attributed to reversible losses related to mass transport and ohmic resistance, which the authors claimed could be lowered to zero if the current was interrupted. In a follow-up paper [31], the same authors showed that cell degradation could indeed be reduced by the periodic reduction of the current, and could decline even further with the periodic interruption of the current. Finally, besides the better energetic efficiency and lower degradation offered by pulsed electrolysis, and the recent interest in decoupling the two half-reactions and produce hydrogen in cycles, pulsed water electrolysis presents yet another important advantage: it helps to prevent gas mixing at low current densities, which is an important safety issue [32]. Since hydrogen produced with renewable sources needs to deal with varying power inputs, the current input can sometimes be so low that the hydrogen production rate falls below the rate at which hydrogen crosses the membrane [33]. In this case, gas crossover becomes a relevant issue, both during PEM [34] and alkaline [35] water electrolysis. Pulses can then be used to reduce the input power without reducing the current (for instance by reducing the duty cycle), hence allowing the current to always remain above the level at which gas crossover becomes an issue [36].

During our own previous research [37], we already studied the use of pulsed voltages during water electrolysis on so-called 3-D electrodes. For such electrodes, the specific objective of applying pulses is to facilitate the evacuation of gas bubbles, which otherwise will remain trapped within their macro-porous open structure. This will in turn reduce their active surface area and increase the ohmic resistance of the cell. More specifically, we reported in Ref. [37] a synergistic effect between the use of such 3-D electrodes and the application of a forced electrolyte flow and a pulsed voltage. For pulse widths on the order of a few milliseconds and an optimal combination of all three parameters, a 2-fold increase in current was obtained.

The objective of the current work is to further discriminate between the effect of pulse width and duty cycle when applying both voltage and current pulses during alkaline water electrolysis. Moreover, as compared to our previous study, which was based on pulsed cyclo-voltammetry, a new experimental approach has been used based on pulsed chrono-amperometry, in order to verify that the previously reported improvement can be sustained for longer periods. Finally, current pulses from 10 s down to 1 ms were analyzed as well through pulsed chrono-potentiometry, and their advantage over voltage pulses was demonstrated.

Materials and methods

The electrodes consisted of a 3-D foam made of an Inconel 625 Ni-alloy (>58% Ni, from Alantum) with a pore diameter of 450 μm and a specific surface area of 7800 m^2/m^3. Their in-plane dimension was 2 × 2 cm, and 2 sheets with a thickness of 1.6 mm each were used. Between these electrodes, there was an anion exchange membrane (Fumasep FAA-3-PK-

130), with a thickness of 130 μm, in order to prevent gas mixing and to allow for a good electric contact between the cathodic and anodic compartments. The membrane was composed of a polyaromatic structure coupled to quaternary ammonium groups [38]. The former is a polymeric backbone, important for mechanical and thermal stability, while the latter is an ion exchange group, essential for ionic conductivity of OH^- [39]. The specific ionic conductivity of this membrane has been reported to be between 4 and 8 mS/cm in 0.5 M NaCl and 25 °C [40]. An electrolyte solution of 1 M KOH was prepared with ultrapure water (18.2 MΩ cm, from Sartorius arium 611) and KOH pellets (86.4%, from VWR chemicals). Before each experiment, nitrogen (Alphagaz™ 1 Azote, N_2 > 99.999%, from AirLiquide) was circulated in the catholyte to remove residual oxygen from the solution. Pumps (Commander ID300/302 from Nidec) were used to create a forced electrolyte flow going upwards through the electrode in flow-by mode, at a pumping rate of 115 L/h. This rate was the maximum one that can be applied using our current set-up, and corresponds to a linear flow rate within the cell of 0,25 m/s. Natural convection was studied as well. All experiments were performed at room temperature, using the same experimental filter-press set-up we already described in detail in previous work [37].

A Solartron Modulab XM Potentiostat was used to apply square-shaped pulses. The voltage pulses had a base and peak voltage of 1.2 V and 2.0 V, respectively, while the current pulses varied from 0 to 0.3 A. The pulse width is defined as the time of a single pulse at which the voltage is on, while the duty cycle is the ratio between the pulse width and the total (on + off) pulse period. All experiments were performed at the same integration period and measurement rate to assure reproducibility. For some experiments, hydrogen gas was collected in a transparent graduated cylinder and its production volume recorded with a video-camera. A linear regression of the volumetric hydrogen production versus time gave the hydrogen production rate (in mL/s) and allowed to calculate the Faraday efficiency. To address the contribution of capacitive processes to the measured current, the constitutive equation for an ideally polarizable electrode (IPE) was used [41]:

$$i_c = \frac{E}{R_s}\exp\left(-t/R_s C_{dl}\right) \quad (1)$$

with E the amplitude of the voltage pulse, R_s the solution resistance, and C_{dl} the double layer capacitance.

Results and discussion

Voltage pulses with a duty cycle of 50%

At first, pulses were applied with a duty cycle of 50% and pulse widths between 1 ms and 100 s. Fig. 1(a) compares the current evolution during on-time for the first applied pulse. It can be seen that the current was always highest during the first milliseconds of the pulse application, after which it gradually decreased with time. As a consequence, the sooner the pulse was stopped, i.e. the shorter the pulse width, the higher the average on-current. Pulses with higher on-times were also a continuation of pulses with lower on-times, which confirms the reproducibility of the experiment. Looking at the time evolution of the off-current in Fig. 1(b), a change in polarization was observed. This is indicative for either a discharge of the electrical double layer or the reversal of the redox reaction. Contrary to the on-current, the temporal evolution of the off-current was not the same for the different pulse widths. It reached lower initial values for higher pulse widths, and it stabilized for pulse widths equal or higher than 100 ms. Fig. 2 shows the resulting average current for these first pulses. It was calculated by integrating both the on- and off-currents over time and normalizing by the pulse period. It can be seen that the combination of a higher on-current with a higher off-current still resulted in an apparently better performance for the shortest pulses: for the first pulse, a pulse width of 1 ms resulted in a more than 2-fold increase in average current as compared to a 100 s pulse, in agreement with our previous work based on pulsed CV.

However, this apparent better performance was not observed over the long term, as the shortest pulses showed a rapid decrease in current. This can be seen in Fig. 3 for a series of both 1 ms and 10 ms pulses. Both the on- and off-currents decreased over time, their difference remaining constant at about 1.4 A. This decrease continued until a stabilization occurred after about 10 s of the experiment. As a result, if the average current of a pulse was measured after 10 s, a decrease in pulse width caused a decrease in average

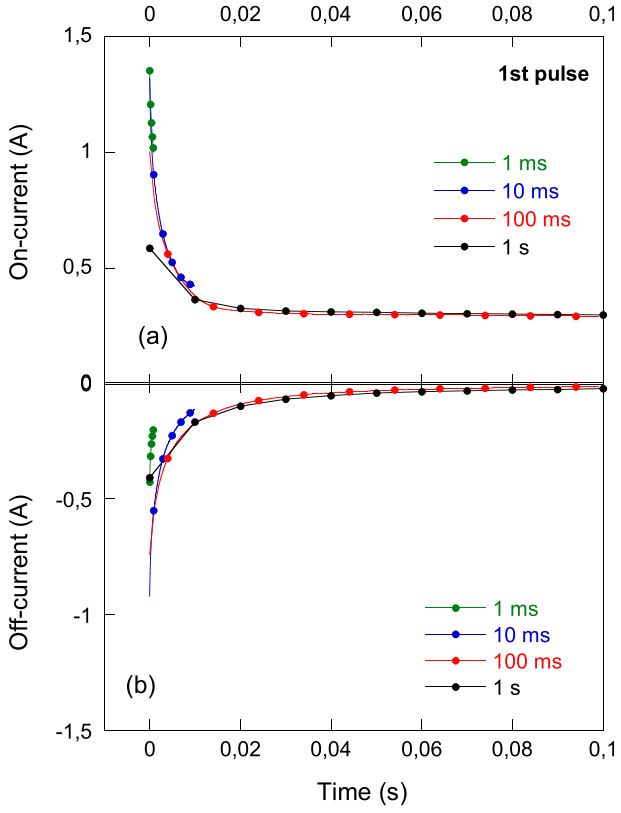

Fig. 1 – Time evolution of the on-current at 2.0 V (a) and off-current at 1.2 V (b) during the first voltage pulse for different pulse widths. Duty cycle of 50%, natural convection.

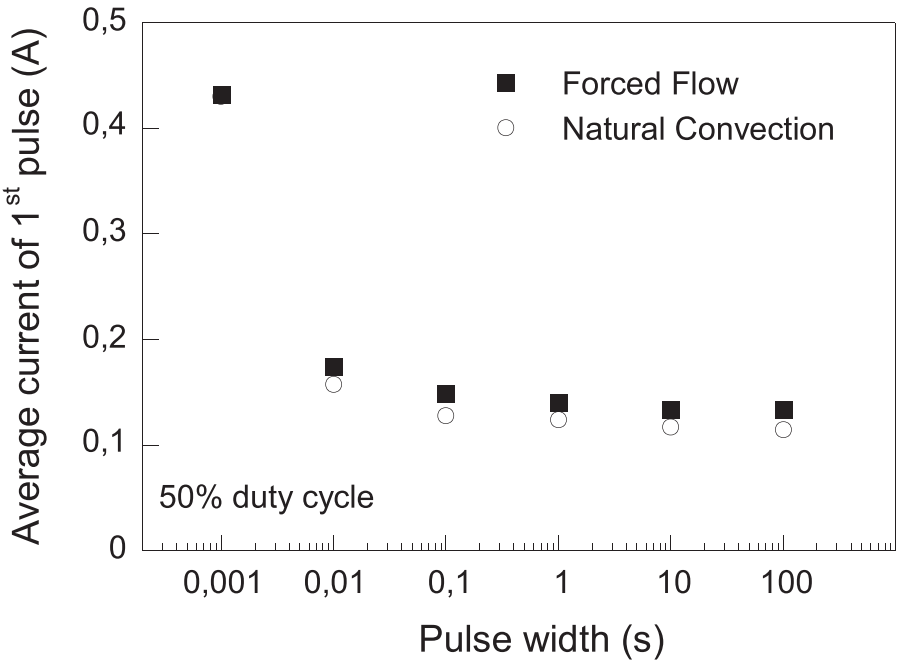

Fig. 2 – Average current of the first voltage pulse as a function of pulse width. Duty cycle of 50%, both natural convection and forced flow.

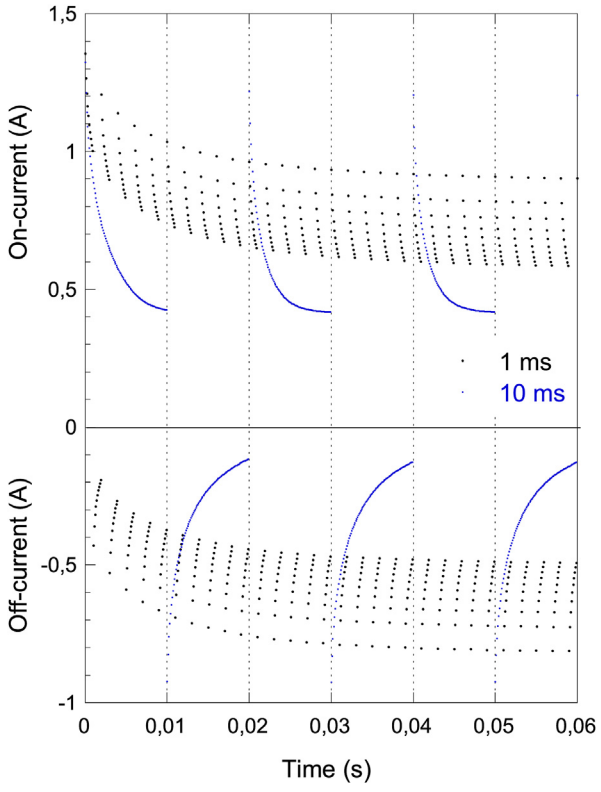

Fig. 3 – Time evolution of the on- and off-current during the first 60 ms for a pulse width of 1 and 10 ms. Duty cycle of 50%, natural convection.

current. This is illustrated in Fig. 4(a), and suggests that for pulse widths lower than 1 s, capacitive processes start to become important. In this respect, the ratio between the charge gained by the system during the pulse on-time and the total charge during a complete period gives an idea of the contribution of faradaic processes. From the results shown in Fig. 4(b), it can be seen that for pulses with a width of 1 ms, only 3% of the on-current was used to conduct faradaic processes. This ratio steeply increased with pulse width until 1 s, where the current was predominantly (>90%) faradaic.

Moreover, no change was observed when comparing the average current in Fig. 4(a) at forced flow and natural convection for a pulse width of 1 ms, while at 10 ms we measured an inversion of the flow effect. This confirms that diffusion was not playing a role anymore, and that almost all the current was capacitive. In other words, the electrical double layer (EDL) was continuously being charged and discharged, so that almost no hydrogen generation took place. Moreover, application of eq. (1) to the current decay curves shown in Fig. 3 allows to provide an estimate of the time constant ($R_s \cdot C_{dl}$) for EDL charging. An average value of 3.2 ms was calculated, confirming the predominance of capacitive processes for pulse widths from 1 to 10 ms.

As to the effect of forced electrolyte flow, it can be seen in Fig. 4(a) that this increases the average current by 12–14% in case faradaic processes are dominant. This can be attributed to an increase in bubble removal rate, or to a decrease in the thickness of the diffusion layer. It also reinforces the idea of a predominance of capacitive processes for the shortest pulses, as in pure capacitive processes there is neither diffusion layer nor bubble formation.

Finally, when comparing our results to the ones from Lin et al. [15], it appears that the enhanced current values reported by the latter during pulsed voltage are probably only the average on-current ones. In that case, similar results were obtained: for pulses with a 50% duty cycle, a pulse periods of 100 ms, and a base and peak voltage of 0 V and 3.5–4.5 V,

respectively, the on-current increased by 10–14%. Maintaining the same conditions and lowering the duty cycle down to 10%, they reported a further increase in on-current of 21–44%, depending on the peak voltage. Therefore, our results clearly demonstrate the need to also include the off-current evolution, since the apparently higher current at on-times can be due to capacitive effects. On the other hand, our results differ from the ones reported by Demir et al. [13]. These authors used transistors to apply voltage pulses, simply blocking any current flow during off-time and hence any change in polarization.

Voltage pulses with a higher duty cycle

In a second stage, the effect of duty cycle was studied. This was done by applying pulses with a short off-time (1 and 10 ms, respectively) and a long total pulse period (from 1 ms to 100 s), resulting in a duty cycle between 50 and 99.9%. The experiment was run for 1000 s to allow for a simultaneous in-situ hydrogen collection as well. The results are shown in Fig. 5 for a fixed pulse off-time of (a) 1 ms and (b) 10 ms, respectively. Comparing both figures indicates that from a duty cycle of 99% onwards, i.e. an on-time which is at least 100 times higher than the off-time, a pulsed voltage signal approaches the DC production rate. Moreover, comparing the measured H_2 production rates (shown on the right-side ordinate in Fig. 5) to the total current response during pulsation, the Faraday efficiency was found under these conditions to be $\geq$ 98%, meaning that almost all the charge was used to produce hydrogen. When looking at the effect of forced flow, the hydrogen production rate was improved by 4–7% for voltage pulses with a 10 ms off-time, as compared to only 0.2 and 4% for a 1 ms off-time. In other words, lower duty cycles (i.e. longer off-times) allow to reinforce the effect of forced flow.

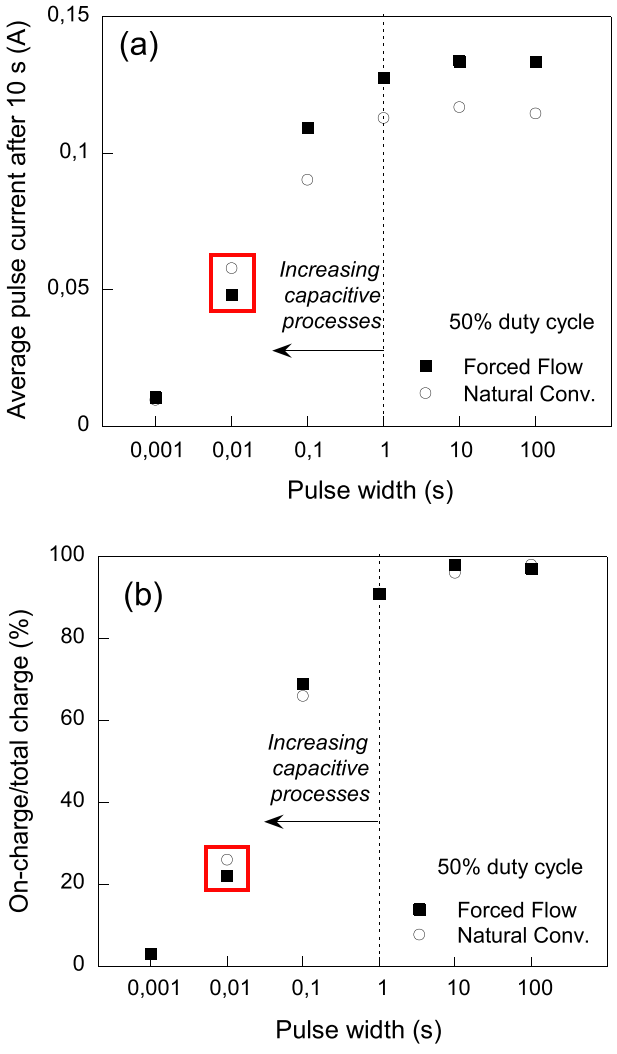

Fig. 4 – (a) Average current after 10 s of experiment as a function of voltage pulse width. For a pulse width of 10 s and 100 s, the second applied pulse was used to calculate the average; (b) Pulse width dependence of the ratio between on-charge and total charge during one voltage pulse period. Duty cycle of 50%, both natural convection and forced flow.

Current pulses with a duty cycle of 50%

As opposed to the application of voltage pulses, there can be no polarity reversal in the case of current pulses when the current is switched back to open-circuit (0 A). The electrical double layer is then being charged at the beginning and never discharged in the course of the experiment. This then allows for a net hydrogen production even at low pulse widths on the order of a few milliseconds. As shown in Fig. 6, after the first pulse, we observed a significant reduction in the cell voltage needed to reach 0.3 A (corresponding to a current density of 0.075 A/cm^2). This is especially the case at high pulse frequencies, and despite the fact that the time evolution of the cell voltage at the beginning of all pulses was similar to DC. Since the duty cycle was the same in all cases (50%), the best pulse configuration was the one with the smallest pulse width (10 ms). In this case, as shown in Fig. 7(a), a reduction in cell potential (averaged over 10 min) on the order of 30 mV was observed in comparison to DC for both natural convection and forced flow. This represents a reduction of 4% in cell overpotential. Also note that DC water electrolysis at 0.3 A was performed before and after the pulse experiment, as illustrated in Fig. 7(b). This was to assure that no modification in the electrode behavior had occurred. In all the cases, the DC behavior was the same at the beginning and the end of each experiment.

When comparing the above results to available literature date, they are in qualitative agreement with the ones from Vincent et al. [28]. These authors reported a reduction in cell potential of 45 mV during the application of 20 ms current pulses from 0 to 0.1 A/cm^2 with a 50% duty cycle. As in our case, they also observed a better performance for pulses with higher frequencies: when decreasing the pulse period from 20 s to 2 ms, a further decrease in cell potential was measured from 45 mV to 540 mV (corresponding to an overpotential reduction of 72%). However, as opposed to the results obtained in Refs. [28], we did not observe any plateau at high pulse periods when plotting the average cell voltage vs. pulse period in Fig. 7(a). Since this plateau can be attributed to the complete establishment of the diffusional

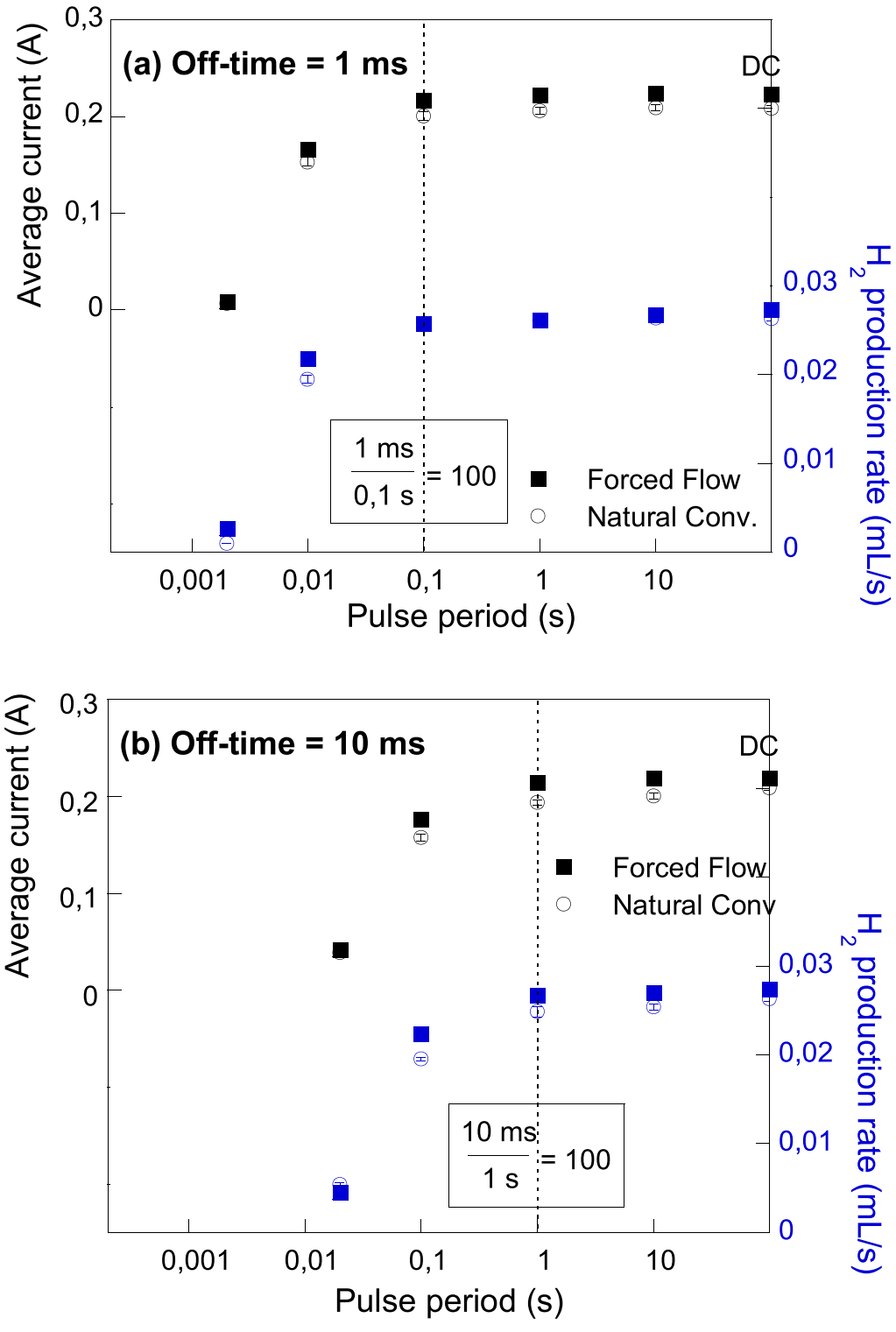

Fig. 5 – Average current (left ordinate) and hydrogen production rate (right ordinate) as a function of voltage pulse period for an off-time of (a) 1 ms and (b) 10 ms. Both natural convection and forced flow.

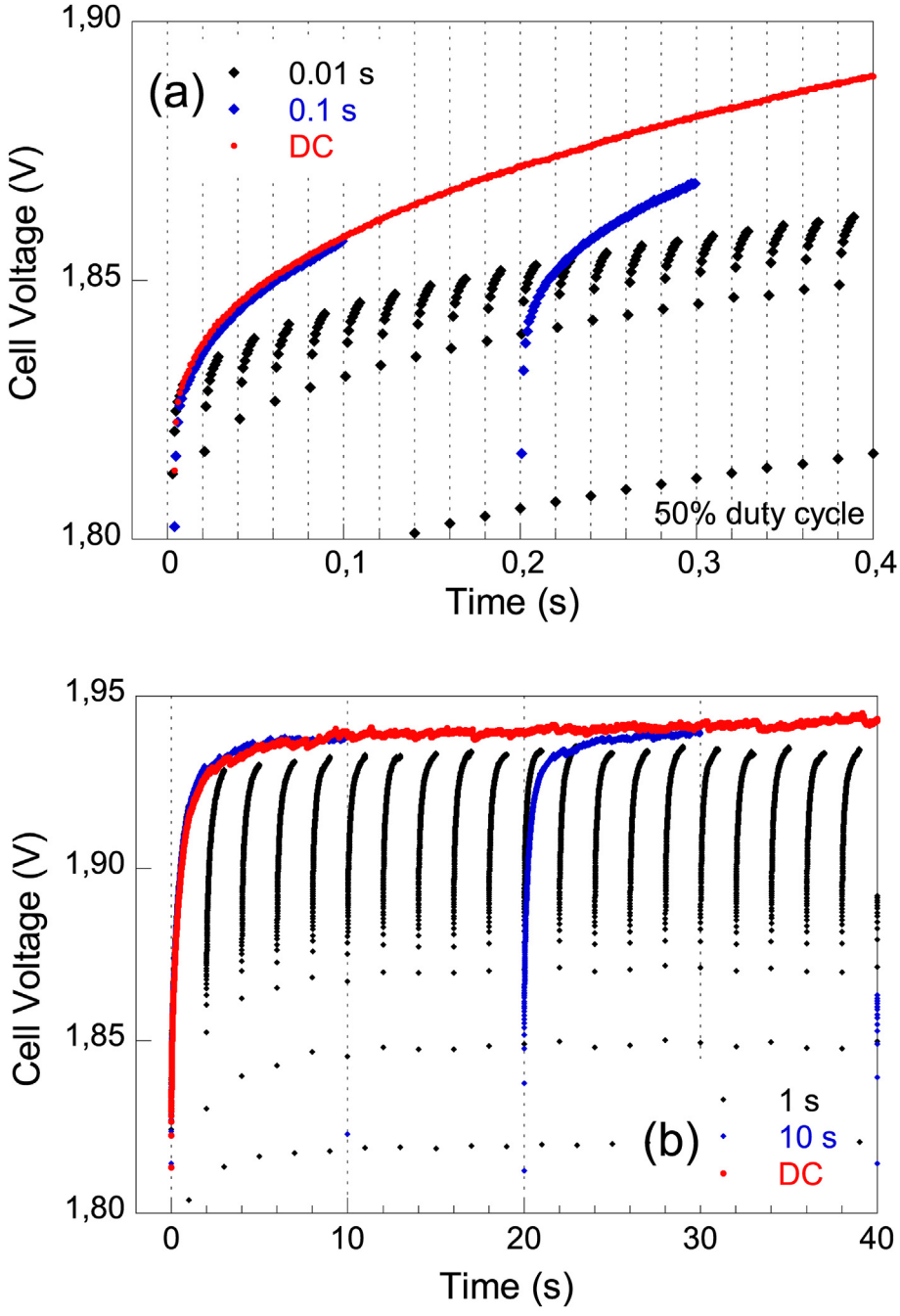

Fig. 6 – Time evolution of the cell voltage for current pulses between 0 and 0.3 A (corresponding to 0,075 A/cm^2) for pulse widths of (a) 0.01 and 0.1 s and (b) 1 and 10 s. The DC behavior at 0.3 A is shown for comparison. Duty cycle of 50%, natural convection.

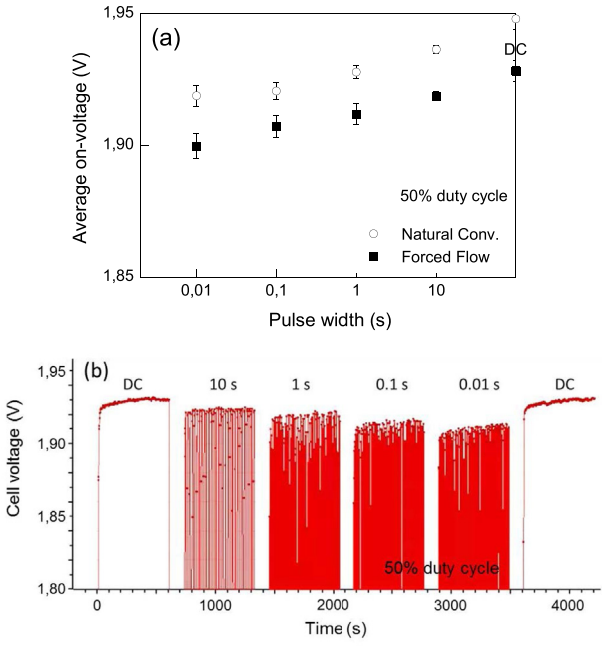

Fig. 7 – (a) Average cell voltage during 10 min of experiment as a function of current pulse width. Duty cycle of 50%, both natural convection and forced flow; (b) Time evolution profile of the cell voltage during a typical pulsed current experiment, showing that the DC behavior measured at the end of each experiment was the same as the one at the beginning.

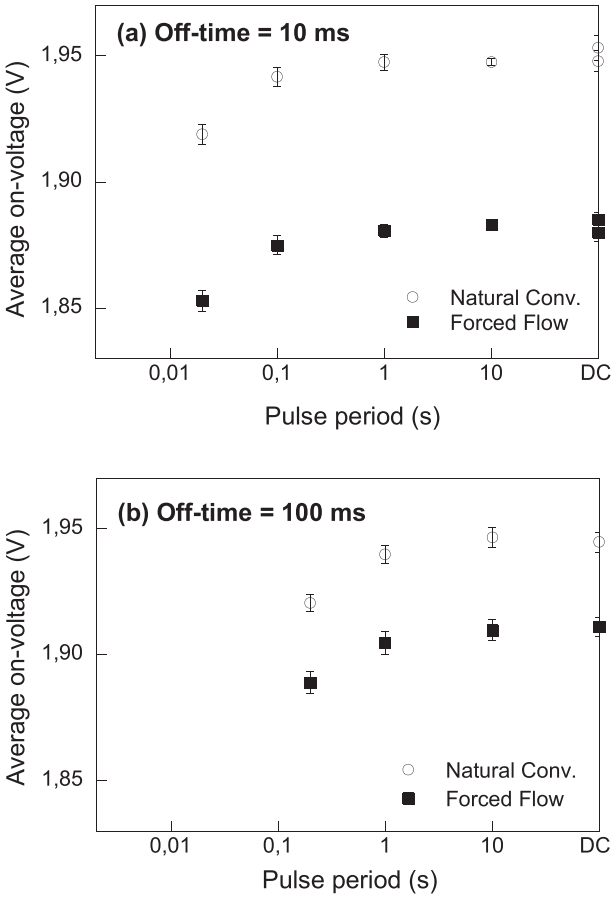

Fig. 8 – Average cell voltage as a function of current pulse period for an off-time of (a) 10 ms and (b) 100 ms. Both natural convection and forced flow.

boundary layer, it also implies that this layer was still not fully established after 10 s in our own experimental set-up.

Current pulses with duty cycles other than 50%

The effect of applying current pulses with duty cycles higher than 50% is shown in Fig. 8. No statistically significant decrease in cell voltage relative to DC could be observed. With the introduction of a forced flow, a reduction in overpotential of 9 and 5% was obtained for current pulses with off-times of 10 and 100 ms, respectively. These results are in line with the conclusions of Eigeldinger et al. [42], who reported that a forced electrolyte flow allows to drastically reduce the bubble coverage of gas evolving electrodes, thereby decreasing the overall cell voltage.

The fact that current pulses only have a statistically significant effect for duty cycles lower than 50% is confirmed in Fig. 9. In this case, the combined effect of low pulse periods with low duty cycles gave the best performance: for a 20% duty cycle and a 2 ms pulse period, we observed a 260 mV (i.e. 28%) reduction in cell overpotential, as opposed to only 17% for a 50% duty cycle. Such increase in performance when decreasing the duty cycle is in line with the observations from Lin et al. [15] in the case of voltage pulses. The effect of lower duty cycles is also beneficial for all pulse periods, but most pronounced for the lower ones (i.e. the highest frequencies). Therefore, our results indicate that the application

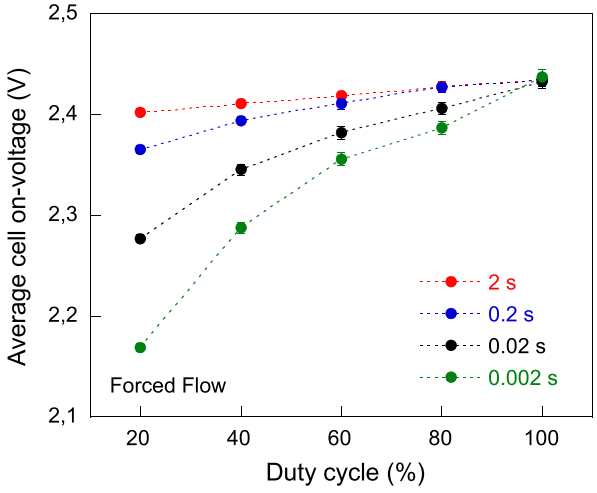

Fig. 9 – Duty cycle dependence of the average cell on-voltage for current pulses with different pulse periods. Peak current of 0.3 A, forced flow.

of current pulses with small pulse periods (ms-range) and low duty cycles (10–20%) can be a promising method for improving the cell performance during alkaline water electrolysis.

Conclusions

In the case of voltage pulses, when considering only the first pulse, the apparent higher average current obtained for a 50% duty cycle at short pulse widths on the order of a few ms was mainly the result of capacitive effects. Once the charge/discharge cycle of the electrical double layer achieves a steady state, such short pulses were not able anymore to provide significant hydrogen generation currents. As a consequence, voltage pulses presented no advantage as compared to conventional DC electrolysis. Current pulses on the other hand are able to block double layer discharging during off-time, as well as the possible reduction of nickel hydroxides at the anode and the oxidation at the cathode. As a result, all the current can be used for hydrogen/oxygen production, and voltage pulses present a better performance than DC electrolysis. For a duty cycle of 50%, the highest reduction in cell overpotential (17%) occurred for the smallest pulse periods (2 ms). In that case, this reduction further increased to 28% when decreasing the duty cycle to 20%. This was attributed to a reduction of the thickness of the diffusion layer and the facilitation of bubble removal. The better performance for current pulses is also an important achievement in the use of water electrolysis for grid balancing, as the power input can be easily changed by a change in the duty cycle. Finally, it was observed that a forced flow of electrolyte enabled to further improve the process efficiency, but only when faradaic processes were dominant.

Declaration of competing interest

The authors declare that they have no known competing financial interests or personal relationships that could have appeared to influence the work reported in this paper.

REFERENCES

[1] Cook J, Oreskes N, Doran PT, Anderegg WRL, Verheggen B, Maibach EW, et al. Consensus on consensus: a synthesis of consensus estimates on human-caused global warming. Environ Res Lett 2016;11:48002. https://doi.org/10.1088/1748-9326/11/4/048002.

[2] Anderson TR, Hawkins E, Jones PD. CO(2), the greenhouse effect and global warming: from the pioneering work of Arrhenius and Calendar to today's Earth System Models. Endeavour 2016;40:178–87. https://doi.org/10.1016/j.endeavour.2016.07.002.

[3] Abe JO, Popoola API, Ajenifuja E, Popoola OM. Hydrogen energy, economy and storage: review and recommendation. Int J Hydrogen Energy 2019;44:15072–86. https://doi.org/10.1016/j.ijhydene.2019.04.068.

[4] Zahnle KJ, Gacesa M, Catling DC. Strange messenger: a new history of hydrogen on Earth, as told by Xenon. Geochem Cosmochim Acta 2019;244:56–85. https://doi.org/10.1016/j.gca.2018.09.017.

[5] Lee JD. Concise inorganic chemistry. 5th ed. New York: John Wiley & Sons; 2008.

[6] Crabtree GW, Dresselhaus MS, Buchanan MV. The hydrogen economy. Phys Today 2004;57:39–44.

[7] Dawood F, Anda M, Shafiullah GM. Hydrogen production for energy: an overview. Int J Hydrog Energy 2020;45:3847–69. https://doi.org/10.1016/j.ijhydene.2019.12.059.

[8] Ursua A, Gandia LM, Sanchis P. Hydrogen production from water electrolysis: current status and future trends. Proc IEEE Feb. 2012;100(2):410–26. https://doi.org/10.1109/JPROC.2011.2156750.

[9] Newman J, Bonino CA, Trainham JA. The energy future. Annu Rev Chem Biomol Eng 2018;9:153–74.

[10] Abdalla AM, Hossain S, Nisfindy OB, Azad AT, Dawood M, Azad AK. Hydrogen production, storage, transportation and key challenges with applications: a review. Energy Convers Manag 2018;165:602–27. https://doi.org/10.1016/j.enconman.2018.03.088.

[11] Vanags M, Kleperis J, Bajars G. Separation of charging and charge transition currents with inductive voltage pulses. Latv J Phys Tech Sci 2011;48:34–40.

[12] Shimizu N, Hotta S, Sekiya T, Oda O. A novel method of hydrogen generation by water electrolysis using an ultra-short-pulse power supply. J Appl Electrochem 2006;36:419–23.

[13] Demir N, Kaya MF, Albawabiji MS. Effect of pulse potential on alkaline water electrolysis performance. Int J Hydrog Energy 2018;43:17013–20.

[14] Huang C. Solar hydrogen production via pulse electrolysis of aqueous ammonium sulfite solution. Sol Energy 2013;91:394–401.

[15] Lin M-Y, Hourng L-W. Effects of magnetic field and pulse potential on hydrogen production via water electrolysis. Int J Energy Res 2014;38:106–16.

[[1][6] Dobó Z, Palotás ÁB. Impact of the current fluctuation on the efficiency of alkaline water electrolysis. Int J Hydrog Energy 2017;42:5649–56.

[17] Dobó Z, Palotás ÁB. Impact of the voltage fluctuation of the power supply on the efficiency of alkaline water electrolysis. Int J Hydrog Energy 2016;41:11849–56.

[18] Chao H-J, Xue D, Jiang W, Li D, Hu Z, Kang J, et al. A low-voltage pulse electrolysis method for the degradation of anthraquinone and azo dyes in chloride medium by anodic oxidation on Ti/IrO2-RuO2-SnO2 electrodes. Water Environ Res 2020;92:779–88. https://doi.org/10.1002/wer.1270.

[19] Othmani A, Kesraoui A, HaneneAkrout, Elaissaoui I, Seffen M. Coupling anodic oxidation, biosorption and alternating current as alternative for wastewater purification. Chemosphere 2020;249:126480. https://doi.org/10.1016/j.chemosphere.2020.126480.

[20] Siracusano S, Trocino S, Briguglio N, Pantò F, Aricò AS. Analysis of performance degradation during steady-state and load-thermal cycles of proton exchange membrane water electrolysis cells. J Power Sources 2020;468:228390. https://doi.org/10.1016/j.jpowsour.2020.228390.

[21] Symes MD, Cronin L. Decoupling hydrogen and oxygen evolution during electrolytic water splitting using an electron-coupled-proton buffer. Nat Chem 2013;5:403–9. https://doi.org/10.1038/nchem.1621.

[22] Mallouk TE. Divide and conquer. Nat Chem 2013;5:362–3. https://doi.org/10.1038/nchem.1634.

[23] Rausch B, Symes MD, Chisholm G, Cronin L. Decoupled catalytic hydrogen evolution from a molecular metal oxide redox mediator in water splitting. Science 2014;345:1326. https://doi.org/10.1126/science.1257443.

[24] Chen L, Dong X, Wang Y, Xia Y. Separating hydrogen and oxygen evolution in alkaline water electrolysis using nickel hydroxide. Nat Commun 2016;7:11741.

[25] Dotan H, Landman A, Sheehan SW, Malviya KD, Shter GE, Grave DA, et al. Decoupled hydrogen and oxygen evolution by a two-step electrochemical–chemical cycle for efficient

overall water splitting. Nat Energy 2019;4:786–95. https://doi.org/10.1038/s41560-019-0462-7.
[26] Bloor LG, Solarska R, Bienkowski K, Kulesza PJ, Augustynski J, Symes MD, et al. Solar-driven water oxidation and decoupled hydrogen production mediated by an electron-coupled-proton buffer. J Am Chem Soc 2016;138:6707–10. https://doi.org/10.1021/jacs.6b03187.
[27] Jin Z, Li P, Xiao D. A hydrogen-evolving hybrid-electrolyte battery with electrochemical/photoelectrochemical charging from water oxidation. ChemSusChem 2017;10:483–8. https://doi.org/10.1002/cssc.201601317.
[28] Vincent I, Choi B, Nakoji M, Ishizuka M, Tsutsumi K, Tsutsumi A. Pulsed current water splitting electrochemical cycle for hydrogen production. Int J Hydrog Energy 2018;43.
[29] Frensch SH, Fouda-Onana F, Serre G, Thoby D, Araya SS, Kær SK. Influence of the operation mode on PEM water electrolysis degradation. Int J Hydrogen Energy 2019;44:29889–98. https://doi.org/10.1016/j.ijhydene.2019.09.169.
[30] Rakousky C, Reimer U, Wippermann K, Carmo M, Lueke W, Stolten D. An analysis of degradation phenomena in polymer electrolyte membrane water electrolysis. J Power Sources 2016;326:120–8. https://doi.org/10.1016/j.jpowsour.2016.06.082.
[31] Rakousky C, Reimer U, Wippermann K, Kuhri S, Carmo M, Lueke W, et al. Polymer electrolyte membrane water electrolysis: restraining degradation in the presence of fluctuating power. J Power Sources 2017;342:38–47. https://doi.org/10.1016/j.jpowsour.2016.11.118.
[32] Grigoriev SA, Millet P, Korobtsev SV, Porembskiy VI, Pepic M, Etievant C, et al. Hydrogen safety aspects related to high-pressure polymer electrolyte membrane water electrolysis. Int J Hydrogen Energy 2009;34:5986–91. https://doi.org/10.1016/j.ijhydene.2009.01.047.
[33] Wallace AG, Symes MD. Decoupling strategies in electrochemical water splitting and beyond. Joule 2018;2:1390–5. https://doi.org/10.1016/j.joule.2018.06.011.
[34] Schalenbach M, Carmo M, Fritz DL, Mergel J, Stolten D. Pressurized PEM water electrolysis: efficiency and gas crossover. Int J Hydrogen Energy 2013;38:14921–33. https://doi.org/10.1016/j.ijhydene.2013.09.013.
[35] Haug P, Koj M, Turek T. Influence of process conditions on gas purity in alkaline water electrolysis. Int J Hydrogen Energy 2017;42:9406–18. https://doi.org/10.1016/j.ijhydene.2016.12.111.
[36] Haug P, Kreitz B, Koj M, Turek T. Process modelling of an alkaline water electrolyzer. Int J Hydrogen Energy 2017;42:15689–707. https://doi.org/10.1016/j.ijhydene.2017.05.031.
[37] de Radiguès Q, Thunis G, Proost J. On the use of 3-D electrodes and pulsed voltage for the process intensification of alkaline water electrolysis. Int J Hydrog Energy 2019;44:29432–40.
[38] Garcia-Herrero I, Alvarez-Guerra M, Irabien A. Electrosynthesis of dimethyl carbonate from methanol and CO2 using potassium methoxide and the ionic liquid [bmim][Br] in a filter-press cell: a study of the influence of cell configuration. J Chem Technol Biotechnol 2016;91:507–13. https://doi.org/10.1002/jctb.4605.
[39] Vincent I, Bessarabov D. Low cost hydrogen production by anion exchange membrane electrolysis: a review. Renew Sust Energ Rev 2018;81:1690–704.
[40] Fuel Cell Store. Technical data sheet - fumasep FAA-3-PK-130 [n.d].
[41] Bard AJ, Faulkner LR. Electrochemical methods : fundamentals and applications. 2nd ed. New York: John Wiley & Sons; 2001.
[42] Eigeldinger J, Vogt H. The bubble coverage of gas-evolving electrodes in a flowing electrolyte. Electrochim Acta 2000;45:4449–56. https://doi.org/10.1016/S0013-4686(00)00513-2.